JOURNAL OF MAGNETIC RESONANCE, Series A 104, 1–9 (1993)

Quantitative Determination of Nonintegral Spin Quadrupolar Nuclei in Solids Using Nuclear Magnetic Resonance Spin-Echo Techniques*

JÜRGEN HAASE† AND ERIC OLDFIELD

Department of Chemistry, University of Illinois at Urbana-Champaign, 505 South Mathews Avenue, Urbana, Illinois 61801

Received September 21, 1992; revised December 22, 1992

Experimental and theoretical results concerning the quantitative determination of non-integral-spin quadrupolar nuclei in static solids using spin-echo nuclear magnetic resonance are presented for the cases of selective, nonselective, and "partially" selective excitation. For a strong quadrupolar coupling, selective excitation of the central $(\frac{1}{2}, -\frac{1}{2})$ transition is shown to give excellent quantitative results on systems of known composition, using both in-phase and 90°-phase-shifted pulse sequences. Off-resonance effects are manifested as intensity oscillations, from which nuclear quadrupole coupling constants may be estimated.

INTRODUCTION

During the past decade, there has been a great increase in use of solid-state nuclear magnetic resonance spectroscopic techniques to investigate non-integral-spin quadrupolar nuclei ($I = \frac{3}{2}, \frac{5}{2}, \ldots, \frac{9}{2}$; e.g. ^{23}Na, ^{17}O, . . . , ^{93}Nb) in inorganic solids, such as minerals, glasses, ceramics, and high-temperature superconductors (*1*). In most cases, valuable information on chemical shifts and nuclear quadrupole coupling constants (e^2qQ/h) has been obtained, and, in some cases, there have been studies of spin–spin (*2*) and spin–lattice (*3*) relaxation. However, in general, there has been little investigation of the topic of signal quantitation.

The presence of a quadrupole interaction is known to complicate NMR intensity measurements (*4*). For example, in powders, the excitation and detection of the wide frequency range of transitions in the spin system may cause errors in intensity measurement, and, due to these difficulties, single-pulse excitation using short pulses is generally thought to be the most reliable method for intensity measurement (*4*). However, in order to improve the resolution of the NMR experiment, other techniques, such as sample spinning and spin-echo experiments, are sometimes necessary, but in and of themselves may complicate intensity measurements even further.

For samples containing relatively narrow lines, one-pulse methods using short nonselective pulses give good quantitative results (*4*). For samples where increased resolution is required and lines are again relatively narrow, one-pulse methods using sample spinning at the "magic angle" are effective, and Massiot *et al.* (*5*) have recently discussed the precautions necessary to obtain good quantitative results, due to the problems associated with the presence of sideband contributions to the observed central transition, as well as the influence of sample rotation during the pulse. The third class of experiments constitutes those in which static samples are used, and radiofrequency excitation is in the form of a two-pulse spin-echo sequence (*2*). Spin-echo techniques are useful for investigating systems with large e^2qQ/h values, where lineshapes would be distorted using conventional one-pulse techniques, and, when combined with the observation that the time constants, T_{2E}, of the spin-echo decays vary widely between different materials (*2*), they offer an alternative way of investigating a wide range of inorganic (and biological) solids. For example, in recent work (*2*), we showed that in the presence of a strong quadrupolar coupling, the spin-echo decay is predictable if the dipolar interactions in the spin system are known. However, we also found the spin-echo amplitude and decay to be strongly dependent on the bandwidth of excitation of the nuclear spin system, and we only reported results on selectively excited central transitions.

We have now investigated the influence of the bandwidth of excitation on the spin-echo decay in more detail, and in this paper we show that reliable intensity measurements can be performed on both simple and complex samples, by using two-pulse spin-echo techniques, under a variety of radiofrequency excitation conditions. For more general background information, we recommend that the reader consult Refs. (*6–8*).

THEORETICAL ASPECTS

We consider spin systems for which the following relation holds:

* This work was supported in part by the United States National Institutes of Health (Grants HL-19481 and GM-40426) and by the United States National Science Foundation Materials Research Laboratory Program (J.H.; Grant DMR 89-20538).

† Supported in part by the Deutsche Forschungsgemeinschaft.

1064-1858/93 $5.00

$$\|\mathcal{H}_Z\| \gg \|\mathcal{H}_Q\| \geq \|\mathcal{H}_D\|. \quad [1]$$

That is, the Zeeman interaction, $\mathcal{H}_Z$, is strong enough that its eigenfunctions are the eigenfunctions of the total Hamiltonian, and the quadrupole interaction, $\mathcal{H}_Q$, exceeds the other internal interactions, in particular the magnetic dipole interaction, $\mathcal{H}_D$, among the spins.

The relevant Hamiltonians describing the interactions in the spin system are given in the interaction representation with respect to the Zeeman interaction, $\mathcal{H}_Z = \hbar\omega_L I_z$, where ω_L is the Larmor frequency of the nuclear spin in the static magnetic field, $B_0 = \omega_L/\gamma$. By applying the Magnus expansion (*9*), we calculate for the quadrupole interaction to first order

$$\mathcal{H}_Q^{(1)} = \frac{\hbar\omega_Q}{6}\sqrt{\frac{2}{3}}[3I_z^2 - I(I+1)]V_0, \quad [2]$$

and to second order, we obtain the secular part

$$\mathcal{H}_{Q_{sec}}^{(2)} = -\frac{\hbar\omega_Q^2}{9\omega_L}\left\{2I_z\left[2I_z^2 - I(I+1) + \frac{1}{4}\right]V_{-1}V_1 + I_z\left[I_z^2 - I(I+1) + \frac{1}{2}\right]V_{-2}V_2\right\} \quad [3]$$

and the nonsecular term

$$\mathcal{H}_{Q_{nsec}}^{(2)} = -\frac{\hbar\omega_Q^2}{18\omega_L}\sqrt{\frac{3}{2}}\{(I_-I_z^2 + 2I_zI_-I_z + I_z^2I_-)V_0V_{+1} - (I_+I_z^2 + 2I_zI_+I_z + I_z^2I_+)V_0V_{-1} - (I_+^2I_z + I_zI_+^2) \times V_0V_{+2} + (I_+^2I_z + I_zI_+^2)V_0V_{-2}\}. \quad [4]$$

In Eqs. [2]–[4], ω_Q denotes the pure quadrupole frequency,

$$\omega_Q = \frac{3e^2qQ}{2I(2I-1)\hbar}, \quad [5]$$

and the quantities V_m denote the irreducible tensor components of the electric field gradient divided by $V_{ZZ}^{(PAS)} \equiv eq$, its largest value in the principal-axis system.

As an example, we have

$$V_0 = \sqrt{\frac{3}{2}}\left\{\frac{3\cos^2\beta - 1}{2} + \frac{\eta}{2}\sin^2\beta\cos 2\alpha\right\}, \quad [6]$$

where we use the Wigner rotation matrices (*10*)

$$V_m = \sum_{m'} D_{m'm}^{(2)}V_{m'}^{(PAS)};$$

$$V_0^{(PAS)} = \sqrt{\frac{3}{2}}; \quad V_{\pm1}^{(PAS)} = 0; \quad V_{\pm2}^{(PAS)} = \frac{\eta}{2}. \quad [7]$$

For a radiofrequency pulse along the y axis (a y pulse), the first-order Hamiltonian in the interaction representation is

$$\mathcal{H}_{RF}^{(1)} = \hbar\omega_{RF}I_y. \quad [8]$$

For the other Hamiltonians we refer the reader to the literature (*9, 11*) since for our numerical calculations, we have explicitly used only the Hamiltonians for the Zeeman, RF field, and quadrupole interaction.

The density operator at a time t is given by

$$\rho(t) = \exp\left\{-\frac{i}{\hbar}\mathcal{H}t\right\}\rho(0)\exp\left\{\frac{i}{\hbar}\mathcal{H}t\right\}, \quad [9]$$

where $\mathcal{H}$ is the sum of the (time-independent) interactions considered in the Magnus expansion. The (demodulated) NMR signal, $F(t)$, is normalized as

$$F(t) = F_0\frac{\mathrm{tr}\{\rho(t)I_+\}}{\mathrm{tr}\{I_x^2\}} \equiv \frac{F_0}{\mathrm{tr}\{I_x^2\}}\langle I_-|\rho(t)\rangle, \quad [10]$$

where

$$F_0 = \frac{N\hbar^2I(I+1)}{3kT}\gamma^3B_0^2. \quad [11]$$

With this normalization, we find for an equilibrium density operator, $\rho(0) = I_z$, that, after a nonselective $\pi/2$ pulse, $F(0) = 1$ if $F_0 = 1$, as commonly used in the literature. The constant factor F_0 in Eq. [11] contains the magnitude of the thermodynamic equilibrium magnetization multiplied by γB_0, since the voltage induced in the RF coil is also proportional to the Larmor frequency. N and I are the number of resonant spins and their spin quantum number, k is the Boltzmann constant, T is the absolute temperature γ is the gyromagnetic ratio, and B_0 is the static magnetic field.

Single-Pulse Experiments

For a single-pulse experiment (Fig. 1A), the intensity of the free induction decay, $F(t = 0)$, follows from Eq. [10] as

$$F(0) = \frac{F_0}{\mathrm{tr}\{I_x^2\}}\sum_{m=-I}^{I-1}2W_m\langle m|\rho(\tau)|m+1\rangle, \quad [12]$$

where

$$W_m = \tfrac{1}{2}\sqrt{I(I+1) - m(m+1)}. \quad [13]$$

For *nonselective excitation*, $\|\mathcal{H}_{RF}\| \gg \|\mathcal{H}_Q\| \geq \|\mathcal{H}_D\|$, $\mathcal{H}_Q$ can be neglected during the pulse, and we have for a y pulse:

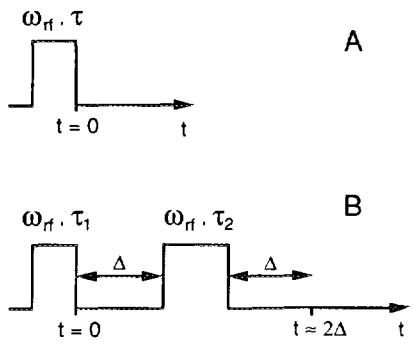

FIG. 1. One- and two-pulse sequences used to record spectra, as described in the text.

$$F^{ns}(0) = \frac{F_0}{\mathrm{tr}\{I_x^2\}} \sum_{m=-1}^{I-1} 2W_m^2 \sin(\omega_{RF}\tau). \qquad [14]$$

Thus, for each transition, as well as for the total intensity, a sinusoidal dependence of the intensity on ω_{RF} and τ is found (*4*). In particular, if the central-transition intensity, $F^{ns}_{-1/2,1/2}$, can be measured separately, it follows that

$$F^{ns}_{-1/2,1/2} = \frac{3(2I+1)}{8I(I+1)} F_0 \sin(\omega_{RF}\tau). \qquad [15]$$

For *selective excitation*, $\|\mathscr{H}_Q\| \gg \|\mathscr{H}_{RF}\| \gg \|\mathscr{H}_Q^{(2)}\|, \|\mathscr{H}_D\|$, and the central transition can be excited selectively. If we keep only $\mathscr{H}_Q^{(1)}$ and $\mathscr{H}_{RF}^{(1)}$ in Eq. [10], the central transition behaves like a spin-$\frac{1}{2}$ system (*4, 11, 12*) and one finds for the central-transition intensity

$$F^{s}_{-1/2,1/2} = \frac{3}{4I(I+1)} F_0 \sin\left\{\left(I+\frac{1}{2}\right)\omega_{RF}\tau\right\}. \qquad [16]$$

Our numerical calculations, which include also $\mathscr{H}_Q^{(2)}$, show that as long as ω_{RF} is larger than the second-order quadrupolar linewidth for the powder, Eq. [16] is a very good approximation to experiment.

Comparison of Eq. [15] and [16] shows that, as long as $\sin\{(I+\frac{1}{2})\omega_{RF}\tau\}$ can be approximated by $(I+\frac{1}{2})\omega_{RF}\tau$ (i.e., for small flip angles), then

$$F^{s}_{-1/2,1/2} = F^{ns}_{-1/2,1/2} = \frac{3(2I+1)}{8I(I+1)} F^{ns}. \qquad [17]$$

In particular, for the relative error to be smaller than 10%, i.e., for

$$(F^{s}_{-1/2,1/2} - F^{ns}_{-1/2,1/2})/F^{ns}_{-1/2,1/2} \leq 0.1,$$

then

$$\omega_{RF}\tau \leq \sqrt{\frac{0.6}{I(I+1)-\frac{3}{4}}} \approx \frac{\pi}{4(I+\frac{1}{2})} \qquad [18]$$

For single-pulse experiments, intensity measurements are correct only as long as the intensity of the central transition can be separated from the whole spectrum or in the case that the total intensity (central plus satellite transitions) can be measured accurately. This is a good approximation either if $\|\mathscr{H}_Q\| \gg \|\mathscr{H}_D\|$ or if $\mathscr{H}_Q$ is very small ($\nu_Q \leq 5$ kHz). However, if the quadrupole interaction is not much larger than the other interactions in the spin system, the amount of satellite-transition intensity in the spectral range of the central transition must be considered, as with the sample-spinning results of Massiot *et al.* (*5*). In this case, spin-echo methods can be very helpful.

Spin-Echo Experiments

By using Eqs. [9]–[11] and the definitions shown in Fig. 1B, the spin-echo amplitude, $E(2\Delta)$, is given by

$$E(2\Delta) = \frac{F_0}{\mathrm{tr}\{I_x^2\}} \left\langle I_- \left| \exp\left\{-\frac{i}{\hbar}\mathscr{H}\Delta\right\} \exp\left\{-\frac{i}{\hbar}P_2\tau_2\right\} \right.\right.$$
$$\left.\left. \times \exp\left\{-\frac{i}{\hbar}\mathscr{H}\Delta\right\} \exp\left\{-\frac{i}{\hbar}P_1\tau_1\right\} \right| I_z \right\rangle, \qquad [19]$$

where $P_{1,2}$ denotes the Hamiltonian during the first and second pulse, respectively, and $\mathscr{H}$ stands for the other interactions in the absence of the RF pulse.

For nonselective excitation, $\|\mathscr{H}_{RF}\| \gg \|\mathscr{H}_Q\|$, however, even if the spin system can be *excited* nonselectively, there may be major problems in recording undistorted signals, due to finite spectrometer dead times, especially when e^2qQ/h (or chemical-shift anisotropy line-broadening) values are large, as is often the case. In these situations, spin-echo methods can greatly improve the accuracy of intensity measurements. Applying, e.g., a nonselective $(\pi/2)|_y - \pi|_y$ pulse sequence, and neglecting any internal interactions during the pulse, we can rearrange the trace in Eq. [19] to yield

$$E(2\Delta) = \frac{F_0}{\mathrm{tr}\{I_x^2\}} \left\langle I_- \left| \exp\left\{-\frac{i}{\hbar}\mathscr{H}\Delta\right\} \right.\right.$$
$$\left.\left. \times \exp\left\{-\frac{i}{\hbar}\mathscr{H}_r\Delta\right\} \right| - I_x \right\rangle, \qquad [20]$$

where

$$\mathscr{H}_r = \exp\{-i\pi I_y\}\mathscr{H} \exp\{i\pi I_y\}. \qquad [21]$$

It follows from Eq. [21] that $\mathscr{H}_Q^{(1)}$ is not changed due to the

π pulse, nor is the Hamiltonian for the homonuclear dipolar interaction. However, Hamiltonians proportional to I_z (e.g., the chemical-shift anisotropy and heteronuclear dipolar interaction) do change their sign. For these interactions, the spin-echo decay will be slower than the free induction decay. A 90°-phase-shifted π pulse gives the same results; only the phase of the echo changes.

If the spin-echo decay due to the other interactions is much slower than the free induction decay due to $\mathscr{H}_Q^{(1)}$, we can again separate the central-transition intensity, $E^{ns}_{-1/2,1/2}$, by choosing pulse distances with $\Delta \gg 1/\nu_Q$, and we then obtain

$$E^{ns}_{-1/2,1/2}(2\Delta) = \frac{1}{\sin(\omega_{RF}\tau)} F^{ns}_{-1/2,1/2} = \frac{1}{\sin(\omega_{RF}\tau)} \frac{3(2I+1)}{8I(I+1)} F^{ns}. \quad [22]$$

For *selective excitation of the central transition*, $\|\mathscr{H}_D\| \ll \|\mathscr{H}_{RF}\| \ll \|\mathscr{H}_Q\|$, and it is generally possible to both selectively excite *and* observe the central transition. If the quadrupole coupling is not known, a nutation experiment can be used to confirm selective excitation by observing the sinusoidal dependence of the intensity on the pulse length. We assume that ω_{RF} is large enough that during the pulses only $\mathscr{H}_Q^{(1)}$ must be retained.

In order to separate $\mathscr{H}_Q^{(1)}$ in the exponential operators from the other much smaller interactions, we use the expression (*13*)

$$\exp\left\{-\frac{i}{\hbar}(A+B)t\right\} = \exp\left\{-\frac{i}{\hbar}At\right\}\exp\left\{-\frac{i}{\hbar} \times \int_0^t \exp\left\{\frac{i}{\hbar}At'\right\} B \exp\left\{-\frac{i}{\hbar}At'\right\} dt'\right\}, \quad [23]$$

where we identify A with $\mathscr{H}_Q^{(1)}$. Due to the structure of the first-order quadrupole interaction, $\mathscr{H}_Q^{(1)} \propto I_z^2$, only certain matrix elements, B_{mn}, survive. For single-spin Hamiltonians, B, we find the restriction $m^2 = n^2$. For the matrix elements B_{mn} of the (two-spin) homonuclear dipolar interaction, $B_{mn} = \langle mm'|\mathscr{H}_D|nn'\rangle$, the nonvanishing elements are $\langle nn'|\mathscr{H}_D|nn'\rangle$ or $\langle n \pm 1n|\mathscr{H}_D|nn \pm 1)\rangle$. This shows that spin flipping is now restricted to a single transition (*2, 14, 15*). With Eq. [23], we can write

$$\exp\left\{-\frac{i}{\hbar}(\mathscr{H}_Q^{(1)} + \bar{\mathscr{H}})t\right\} = \exp\left\{-\frac{i}{\hbar}\mathscr{H}_Q^{(1)}t\right\} \times \exp\left\{-\frac{i}{\hbar}\bar{\mathscr{H}}t\right\} = \exp\left\{-\frac{i}{\hbar}\bar{\mathscr{H}}t\right\}\exp\left\{-\frac{i}{\hbar}\mathscr{H}_Q^{(1)}t\right\} \quad [24]$$

since $\mathscr{H}_Q^{(1)}$ and $\bar{\mathscr{H}}$ commute.

From Eq. [24], we have, for the selectively excited spin-echo decay (Eq. [19]),

$$E^s(2\Delta) = \frac{F_0}{\mathrm{tr}\{I_x^2\}} \left\langle I_- \left| \exp\left\{-\frac{i}{\hbar}\bar{\mathscr{H}}\Delta\right\}\exp\left\{-\frac{i}{\hbar}\bar{\mathscr{H}}_{RF}\tau_2\right\} \times \exp\left\{-\frac{i}{\hbar}\bar{\mathscr{H}}\Delta\right\}\exp\left\{-\frac{i}{\hbar}\bar{\mathscr{H}}_{RF}\tau_1\right\} \right| I_z \right\rangle, \quad [25]$$

where we use the fact that $\exp\{-(i/\hbar)\mathscr{H}_Q^{(1)}t\}|I_z\rangle \equiv \exp\{-(i/\hbar)\mathscr{H}_Q^{(1)}t\} I_z \exp\{(i/\hbar)\mathscr{H}_Q^{(1)}t\} = I_z$. We can again rewrite Eq. [25] using the transformation

$$\bar{\mathscr{H}}_r = \exp\left\{-\frac{i}{\hbar}\bar{\mathscr{H}}_{RF}\tau_2\right\}\bar{\mathscr{H}}\exp\left\{+\frac{i}{\hbar}\bar{\mathscr{H}}_{RF}\tau_2\right\} \quad [26]$$

and find

$$E^{sel}(2\Delta) = \frac{F_0}{\mathrm{tr}\{I_x^2\}} \left\langle I_- \left| \exp\left\{-\frac{i}{\hbar}\bar{\mathscr{H}}\Delta\right\}\exp\left\{-\frac{i}{\hbar}\bar{\mathscr{H}}_r\Delta\right\} \times \exp\left\{-\frac{i}{\hbar}\bar{\mathscr{H}}_{RF}\tau_2\right\}\exp\left\{-\frac{i}{\hbar}\bar{\mathscr{H}}_{RF}\tau_1\right\} \right| I_z \right\rangle. \quad [27]$$

Since $\mathscr{H}_{RF} \propto I_{x,y}$, only two matrix elements form $\bar{\mathscr{H}}_{RF}$, the off-diagonal elements $\langle \pm\frac{1}{2}|I_{x,y}|\mp\frac{1}{2}\rangle = (I+\frac{1}{2})\langle \pm\frac{1}{2}|S_{x,y}|\mp\frac{1}{2}\rangle$, where $S_{x,y}$ are spin-$\frac{1}{2}$ angular momentum operators.

As an example, if $\omega_{RF}\tau = [1/(I+1/2)](\pi/2)$, we have for a selective y pulse, $\bar{\mathscr{H}}_{RF}\tau = (\pi/2)S_y$, and

$$\exp\left\{-\frac{i}{\hbar}\bar{\mathscr{H}}_{RF}\tau\right\}|I_z\rangle = |S'_x\rangle. \quad [28]$$

The prime means that for $|m| > \frac{1}{2}$, $\langle m|S'_x|n\rangle = m\delta_{m,n}$, and, for $|m| = \frac{1}{2}$, $\langle m|S'_x|n\rangle = \langle m|S_x|n\rangle$. A pulse for which Eq. [28] holds we call a selective $\pi/2$ pulse.

We now consider an in-phase selective $\pi/2|_y - \pi|_y$ pulse sequence. From Eq. [27] it follows that the spin-echo amplitude is given by

$$E^s(2\Delta) = \frac{F_0}{\mathrm{tr}\{I_x^2\}} \left\langle I_- \left| \exp\left\{-\frac{i}{\hbar}\bar{\mathscr{H}}\Delta\right\} \times \exp\left\{-\frac{i}{\hbar}\bar{\mathscr{H}}_r\Delta\right\} \right| -S'_x \right\rangle. \quad [29]$$

We recently calculated the second moment for such a spin-echo decay in the presence of a magnetic dipole interaction (*2*). For absolute intensity measurements, we must assume that the spin-echo decay due to dipolar interactions is small, which is often true for strong quadrupolar coupling (*2*). For the normalization of Eq. [29], we consider now that $\bar{\mathscr{H}} = \mathscr{H}_Q^{(2)}$, only. From Eqs. [3] and [4] it can be seen that

$$\bar{\mathscr{H}} \equiv \bar{\mathscr{H}}_Q^{(2)} = \bar{\mathscr{H}}_{Q\,sec}^{(2)} = \mathscr{H}_{Q\,sec}^{(2)}. \quad [30]$$

The nonsecular part of the second-order quadrupolar interaction has no matrix elements in either one of the two diagonals. For the transformed Hamiltonian, $\bar{\mathscr{H}}_r$, of Eq. [26], we thus must consider

$$\mathscr{H}^{(2)}_{\mathrm{Q\,sec\,r}} = \exp\left\{-\frac{i}{\hbar}\pi S_y\right\}\mathscr{H}^{(2)}_{\mathrm{Q\,sec}}\exp\left\{+\frac{i}{\hbar}\pi S_y\right\}. \quad [31]$$

Now, the selective π pulse inverts only the diagonal elements of $\mathscr{H}^{(2)}_{\mathrm{Q\,sec}}$ with $|m| = \frac{1}{2}$ and leaves the elements with $|m| > \frac{1}{2}$ unchanged. Since $\mathscr{H}^{(2)}_{\mathrm{Q\,sec\,r}}$ and $\mathscr{H}^{(2)}_{\mathrm{Q\,sec}}$ still commute, their sum represents a diagonal matrix with no central elements. Consequently, we find with use of Eq. [29] that

$$E^{\mathrm{s}}(2\Delta) = -\frac{F_0}{\mathrm{tr}\{I_x^2\}}\langle I_-|S'_x\rangle \equiv -\frac{F_0}{\mathrm{tr}\{I_x^2\}}\mathrm{tr}\{I_+S'_x\}$$

$$= -\frac{F_0(I+\frac{1}{2})}{\mathrm{tr}\{I_x^2\}}\mathrm{tr}\{S_+S_x\}. \quad [32]$$

It can be seen from Eq. [32] that, as expected, only the central transition contributes to the spin-echo intensity, and using $\mathrm{tr}\{I_x^2\} = \frac{1}{3}I(I+1)(2I+1)$ we find that

$$E^{\mathrm{s}}(2\Delta) = E^{\mathrm{s}}_{-1/2,1/2} = -\frac{3F_0}{4I(I+1)}$$

$$= \frac{-1}{\sin\{(I+\frac{1}{2})\omega_{\mathrm{RF}}\tau\}}F^{\mathrm{s}}_{-1/2,1/2}. \quad [33]$$

Since in Eq. [31] the phase of the selective π pulse is of no importance, and a 90° phase shift between the two pulses changes only the initial state (Eq. [29]) to S'_x compared to $-S'_x$, a 90°-phase-shifted selective pulse ($\pi/2|_y - \pi|_x$) sequence does not change the results of Eqs. [32] and [33].

Using these basic results, we discuss below the effects of selective and nonselective excitation on signal quantitation in a variety of inorganic solids.

EXPERIMENTAL METHODS

^{27}Al NMR measurements were made using a "homebuilt" spectrometer, which operates using an Oxford Instruments (Osney Mead, UK) 11.7 T, 2.0 in. bore superconducting solenoid magnet, a Nicolet (Madison, Wisconsin) Model 1280 computer interfaced to a Nicolet Model 2090-IIIC (Explorer) transient recorder, and either Amplifier Research (Souderton, Pennsylvania) or Henry Radio (Los Angeles, California) radiofrequency amplifiers. Static probes were of a homebuilt solenoidal coil design. The length of the sample was less than one-third the length of the RF coil, in order to reduce RF inhomogeneity effects. The MAS probe was a homebuilt dual-bearing (WINDMILL) design.

Upon changing samples, the probe was always tuned and matched to a 50 ohm load. The radiofrequency field strength, ω_{RF}, was determined initially by using a very small sample (~5 μl) of aqueous $AlCl_3$ and was then routinely adjusted by varying the transmitter power level, since $\omega_{\mathrm{RF}} \propto \sqrt{QP} \propto \sqrt{QU}$, where Q is the quality factor of the probe (~70), P the transmitter power, and U the RF amplitude. We found (using the $AlCl_3$ standard) $\omega_{\mathrm{RF}} \propto U$ to be very accurate over the entire range of ω_{RF} we have used. Q was kept relatively low, in order to minimize Q differences upon changing from one sample to another. Selective excitation of the central transition was also routinely checked for each sample by recording the signal intensity as a function of the pulse width (*2, 4, 12*).

The Al_2O_3 (corundum) powder was from Fisher Scientific (Fair Lawn, New Jersey), and γ-Al_2O_3 was from Alfa (Johnson Matthey, Ward Hill, Massachusetts). The zeolites NaA and NaY were the gift of Dr. E. Flanigen (Union Carbide Corp., Tarrytown, New York). H^+–ZSM-5 was from Bruce Calvert at Mobil (Mobil Research and Development Corp., Princeton, New Jersey).

RESULTS AND DISCUSSION

We now discuss our experimental results on one- and two-pulse (spin-echo) excitation of non-integral-spin quadrupolar nuclei in solids. In this paper, we will only consider results for static samples. The reason for this is that we are particularly interested in investigating formulated, real-world zeolite catalysts, which typically contain very large amounts of nonframework Al in the form of various binders—aluminas, silica aluminas, clays, and so forth. Under conditions of "magic-angle" sample spinning, both octahedral and tetrahedral (and perhaps other binder coordination geometry) Al signals tend to completely mask the small but important signals from framework zeolitic sites involved in catalysis. Figure 2A shows a typical 11.7 T ^{27}Al MAS NMR spectrum of a physical mixture containing H^+–ZSM-5 and γ-Al_2O_3. As can be seen in Fig. 2A, there are very large signals from the octahedral and tetrahedral sites in the γ-Al_2O_3 phase, while the signal from the framework Al in the ZSM-5 zeolite is more difficult to identify (or quantitate), since it is obscured by the large tetrahedral-Al γ-Al_2O_3 signal (at ~65 ppm). However, simply stopping sample rotation (data not shown) causes a much better discrimination between the (broad) γ-Al_2O_3 and (narrow) ZSM-5 zeolite resonances. Moreover, as shown in Fig. 2B, it is a straightforward matter to completely edit away all γ-Al_2O_3 features, by use of a selective $\pi/2$—π pulse sequence, because of the short T_2 of the γ-Al_2O_3 phase. We are interested in how such spectral-editing processes can best be carried out and how spin quantitations are affected and will consider briefly first some one-pulse results, followed by a detailed analysis of the use of two-pulse spin-echo NMR for spin quantitation.

Single-Pulse Experiments

Quantitation of NMR intensity using single-pulse experiments is known to give reliable results for both static and

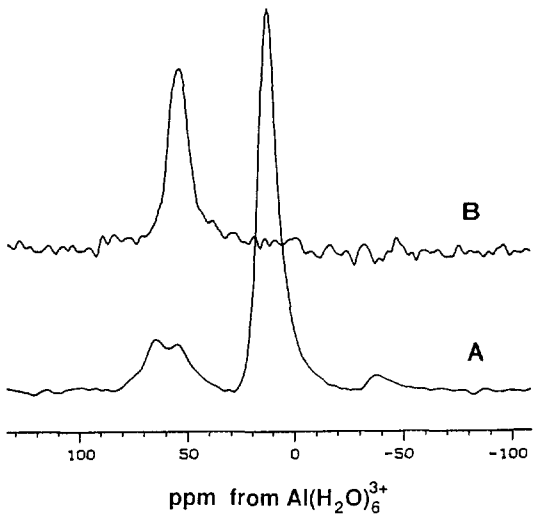

FIG. 2. The 11.7 T ^{27}Al NMR spectra of a physical mixture of H^+-ZSM-5 (70:1, Si/Al) plus γ-Al_2O_3. The ratio of Al nuclei in the zeolitic and γ-Al_2O_3 structure was about 1:160. (A) 6.2 kHz MAS, 1 μs 90° pulse excitation, 600 scans, 150 Hz line broadening due to Gaussian multiplication. (B) Static, 40 μs ($\pi/2$)—80 μs (π) pulse excitation, 50,000 scans, 150 Hz line broadening due to Gaussian multiplication. The recycle time was 0.2 s in both cases.

magic-angle spinning experiments (*4, 5*). Small flip angles are typically applied in order to compare species with different quadrupolar couplings (cf. Eqs. [17] and [18]). However, since small flip angles, $\omega_{RF}\tau < \pi/[4(I + \frac{1}{2})]$, are required, signal-to-noise problems may arise. As we show in Fig. 3 for corundum powder, numerical simulations of the nutation experiments recorded at different RF amplitudes can improve the reliability of the quantitation. An overall good agreement is observed in Fig. 3, by fitting the experimental dependencies with one intensity parameter, F_0^{ex} (cf. Eqs. [10] and [11]), and using ν_Q = 360 kHz, η = 0 (*16, 17*). We compared F_0^{ex} with F_{01}^{ex}, the intensity parameter obtained from the nutation experiment of a standard sample of aqueous $AlCl_3$ (●), since it follows from Eq. [16], with $I = \frac{5}{2}$, that

$$F_0^{ex} = \frac{3}{4I(I+1)} F_{01}^{ex} = \frac{3}{35} F_{01}^{ex}. \qquad [34]$$

We find F_0^{ex} within 5% of the expected intensity as determined from the weight of Al_2O_3 used, while for experiments with a small flip angle, the uncertainty is about 15%. If the quadrupole interaction is not known and the simulation of the nutation experiment is not successful (e.g., there is a broad distribution of quadrupole frequencies), the RF amplitude can be lowered until selective excitation is achieved [cf. Fig. 2 (+)]. Then, the intensities can once again be compared directly and good quantitation obtained.

Spin-Echo Experiments

As we outlined in the Introduction, there are a number of situations in which single-pulse experiments, with or without magic-angle spinning or other techniques, can be expected to give poor quantitative results. For example, for very large e^2qQ/h values, receiver dead-time problems cause spectral distortions. A second type of problem which may be encountered is when there are dynamic range problems or accidental spectral overlaps, in which case, if T_{2E} values are sufficiently different, spin-echo methods can be used to differentiate between different chemical species.

If a nonselective excitation of the spin system can be performed, but substantial inhomogeneous line broadening prevents single-pulse experiments from being reliable, a $\pi/2$—π spin-echo experiment can improve intensity measurements (cf. Eq. [22]). For example, as we reported recently (*18*), we could quantitate ^{11}B in a metallic semiconductor when the ^{11}B resonance was broadened by a small quadrupole interaction ($\nu_Q \approx 6$ kHz) together with a fairly broad distribution of isotropic Knight shifts ($\delta\nu \approx 3$ kHz). Since the nonselective π pulse refocused the distribution of resonance frequencies, while the dipolar linewidth was only about 25 Hz, the ^{11}B spin echo could be used for accurate boron quantitation by comparison with a standard sample of aqueous boric acid [cf. Ref. (*18*)].

For the spin-echo experiments reported here, with selective excitation of the central transition, we used pulses such that

$$\omega_{RF}\tau_1 = \frac{1}{I+\frac{1}{2}}\frac{\pi}{2} \quad \text{and} \quad \omega_{RF}\tau_2 = \frac{1}{I+\frac{1}{2}}\pi. \qquad [35]$$

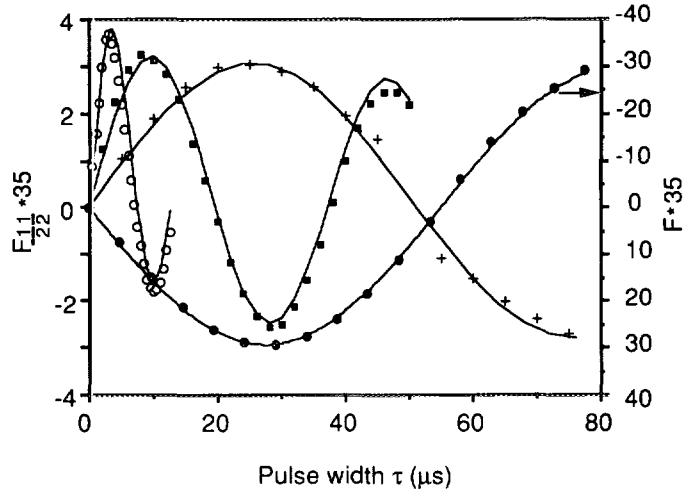

FIG. 3. The 11.7 T ^{27}Al NMR nutation experiments for a corundum powder (α-Al_2O_3) and aqueous $AlCl_3$. ○, ■, +, corundum powder with $\omega_{RF}/2\pi$ of 27.8, 9.1, and 3.3 kHz, respectively; ●, $AlCl_3$ with $\omega_{RF}/2\pi$ of 8.9 kHz. The solid lines represent the corresponding numerical simulations with ν_Q = 360 kHz, η = 0 for corundum and ν_Q = 0 for the liquid. Note that the phase of the liquid line is inverted, for visual clarity.

The spin echo was recorded starting at a time $t = 2\Delta$. Each spin-echo amplitude was determined from the intensity of the phase-corrected Fourier-transformed spectrum.

In order to demonstrate the applicability of the spin-echo technique to the quantitative analysis of a complex system, we chose to investigate a mixture of corundum (α-Al_2O_3) and Linde A zeolite. The sample had a 300-fold excess of ^{27}Al in the corundum phase, which made accurate detection of the minority phase using one-pulse techniques difficult. However, since the selective spin-echo decay for ^{27}Al in zeolite NaA is $\sim$750 μs (*2*) while that of corundum is only $\sim$140 μs (*2*), they could easily be separated in the spin-echo experiment and both phases independently quantitated.

We thus first tuned to the ^{27}Al nuclei in corundum and recorded the spin-echo decay. Then, we tuned to the ^{27}Al nuclei in Linde A zeolite (hydrated, $\nu_Q \approx 165$ kHz) and again recorded the spin-echo decay. The longer the pulse distance Δ, the better the separation of the two components. Results are shown in Fig. 4.

After demonstrating selective excitation of both phases, we obtained an experimental corundum-to-NaA zeolite ^{27}Al ratio of 284:1, in excellent accord with the known composition.

We now consider the effects of spin-echo excitation using *partially selective excitation*, $\|\mathcal{H}_Q\| \geq \|\mathcal{H}_{RF}\|$, and resonance offset effects—both of which may lead to errors in spin quantitation if not accounted for.

For spin-echo experiments, we again used pulses according to Eq. [35]. The spin echoes were recorded, starting at a time $t = 2\Delta$, and each spin-echo amplitude was determined from the phase-corrected Fourier-transformed spectrum. In Fig. 5 we show the spin-echo intensity (in-phase pulse sequence) for NaY zeolite (hydrated) as a function of the pulse distance, Δ, for three different RF amplitudes and the corresponding intensities of the one-pulse free induction decays. As can be seen from Fig. 5, the spin-echo amplitude and decay depend strongly on the RF amplitude, and severe oscillations can be observed if a resonance offset is applied (●, ○). Since we used an in-phase spin-echo sequence, the spin-echo amplitude for the smallest pulse separation used, $\Delta \approx 0.1$ μs, should be approximately equal to the intensity of the free induction decay, $|F_{-1/2,1/2}[\omega_{RF}(\tau_1 + \tau_2)]|$. We have calculated $F_{-1/2,1/2}$ numerically for the different RF amplitudes and pulse widths using the first-order quadrupole interaction only, with $\nu_Q = 270$ kHz and $\eta = 0.5$ (see below). Both the experimental results (cf. Fig. 5) and the numerical results are shown in Table 1. Considering the number of sources of error (determination of ω_{RF}, pulse imperfections at higher power levels, the actual magnitude of the quadrupole interaction, influence of satellite transition intensity present in the range of the central transition), we believe the agreement shown in Table 1 is relatively good.

For $\Delta > 0$ and $\Delta \leq 1/\nu_Q$, it is known that the intensity of the central transition is influenced by the polarization of the satellite transitions, created by the first pulse (*2, 16, 19*), in addition to ordinary satellite-transition intensity. As a result, oscillations of the central-transition intensity arise which complicate the spin-echo decay for small pulse distances. All these effects can be calculated numerically, considering the quadrupole interaction to first order in the powder average, but since $1/\nu_Q$ is a relatively small number, for the spin-echo experiment we neglect these effects by considering only spin echoes with $\Delta \gg 1/\nu_Q$.

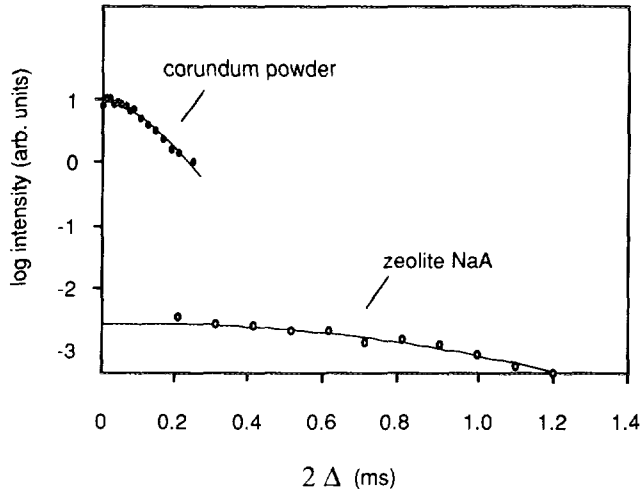

FIG. 4. The 11.7 T ^{27}Al NMR spin-echo decay for a mixture of corundum powder (α-alumina) and hydrated Linde A; ratio of ^{27}Al nuclei, 0.0033:1 for NaA and corundum, respectively. Static sample, in-phase selective $\pi/2$—π pulse sequences, $\omega_{RF} = (2\pi)3.3$ kHz and $\omega_{RF} = (2\pi)0.8$ kHz for corundum and NaA, respectively.

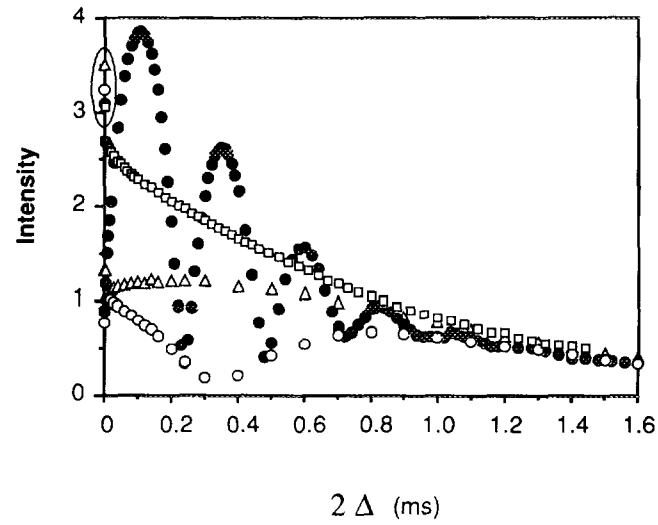

FIG. 5. The 11.7 T ^{27}Al NMR free induction decay and spin-echo results on hydrated Linde Y, at 23°C. In-phase spin-echo experiments with $\omega_{RF}\tau_1 = \pi/6$, $\omega_{RF}\tau_2 = \pi/3$; resonance offset, $\delta\omega$. □, $\omega_{RF} = (2\pi)1.85$ kHz, $\delta\omega = 0$; Δ, $\omega_{RF} = (2\pi)13.9$ kHz, $\delta\omega = 0$; ○, $\omega_{RF} = (2\pi)27.8$ kHz, $\delta\omega = 0$; ●, $\omega_{RF} = (2\pi)27.8$ kHz, $\delta\omega = (2\pi)8.2$ kHz. Circled symbols, free-induction decay results, $\omega_{RF}\tau_1 = \pi/6$. For normalization, cf. Table 1.

TABLE 1
Comparison beween Experimental and Theoretical Signal Intensities Using One- and Two-Pulse Methods

RF amplitude $\nu_{RF} = \omega_{RF}/2\pi$ (kHz)	$\omega_{RF}\tau_1$		$\omega_{RF}(\tau_1 + \tau_2)$	
	a	b	c	b
1.85	3.06	3.06[d]	2.7	2.8
13.9	3.5	3.5	1.3	1.8
27.8	3.3	3.9	0.7	0.6

Note. Experimental and theoretical intensities of the free induction decay of Linde NaY (hydrated) as a function of RF field strength, ω_{RF}, for two different pulse lengths. (Column a) Experiment, one pulse, $\omega_{RF}\tau_1 = \pi/6$. (Column b) Theoretical value. (Column c) Experiment, two pulse, $\omega_{RF}(\tau_1 + \tau_2) = \pi/2$, $E_{-1/2,1/2}$, $(2\Delta = 0)$. (Note d) The experimental and theoretical intensities of the free induction decay for $\nu_{RF} = 1.85$ kHz were used for normalization of all experimental data (Fig. 5). The theoretical results were obtained from numerical calculations by using a first-order quadrupole interaction having $\nu_Q = 270$ kHz, $\eta = 0.5$, and the above RF amplitudes. For selective excitation, $b = \frac{1}{35}|F^z_{-1/2,1/2}|$ (cf. Eq. [16]).

For times $\Delta \sim T_2$, the influence of the dipolar interactions must be considered in any numerical simulation. In contrast to a nutation experiment, where spins are locked along the RF field, in a spin-echo experiment, dipolar dephasing of the magnetization takes place between pulses. The first pulse creates only a central-transition free induction decay, with magnetization left in the $z(B_0)$ direction. The second pulse, at a time $t = \Delta$, to some extent refocuses the first free induction decay, but it also creates a second free induction decay, starting at $t = \Delta$, due to magnetization left in the z direction after the first pulse. At a time $t = 2\Delta$, when the echo forms, the spin-echo amplitude and the second free induction decay are superimposed. Since the second free induction decay has the time constant (T_2) of an ordinary single-pulse response, while the spin-echo decay time constant (T_{2E}) can be very different from T_2, a complicated overall decay is observed experimentally, as can be seen in Fig. 5.

Now, if we apply a resonance offset, $\delta\omega$, this second free induction decay can be investigated separately, since, although the spin echo is not affected by the resonance offset, the phase of the second free induction decay (at $t = 2\Delta$) varies with $\delta\omega\Delta$. Thus, the total signal amplitude displays a pronounced oscillatory behavior, as can be seen in Fig. 5. In order to simulate this oscillatory spin-echo decay, we have used a semiempirical approach, since the numerical calculations become very lengthy when dipolar interactions are included. We have thus calculated the (complex valued) spin-echo amplitude, $E_{-1/2,1/2}(2\Delta)$, considering both the first-order quadrupole interaction and the resonance offset, $\delta\omega$. The result on NaY zeolite for an in-phase pulse sequence (Eq. [35]) having $\omega_{RF} = (2\pi)27.8$ kHz, $\delta\omega = (2\pi)8.2$ kHz is shown in Fig. 6A. Since the oscillations are damped due to the second free induction decay, we separate them by subtracting the time average (mean value), $\bar{E}_{-1/2,1/2}(2\Delta)$, from $E_{-1/2,1/2}(2\Delta)$. We find $|\bar{E}_{-1/2,1/2}(2\Delta)| = 2.04/35$ and, for the amplitude of the oscillation, about the same number, at $\omega_{RF} = (2\pi)27.8$ kHz. The oscillations then decay as the ordinary free induction decay of the ^{27}Al NMR in hydrated NaY zeolite, which is an almost Gaussian decay having $T_2 \approx 240$ μs. This time constant refers to the Δ time scale, rather than to 2Δ, as generally used for T_{2E}. The constant part, $\bar{E}_{-1/2,1/2}(2\Delta)$, will decay with $T_{2E} \approx 800$ μs (Lorentzian decay; cf. Fig. 5). This is shown in Fig. 6B. Since the phases of the experimentally observed signals vary, we compare in Fig. 6C the absolute intensities, as determined from the

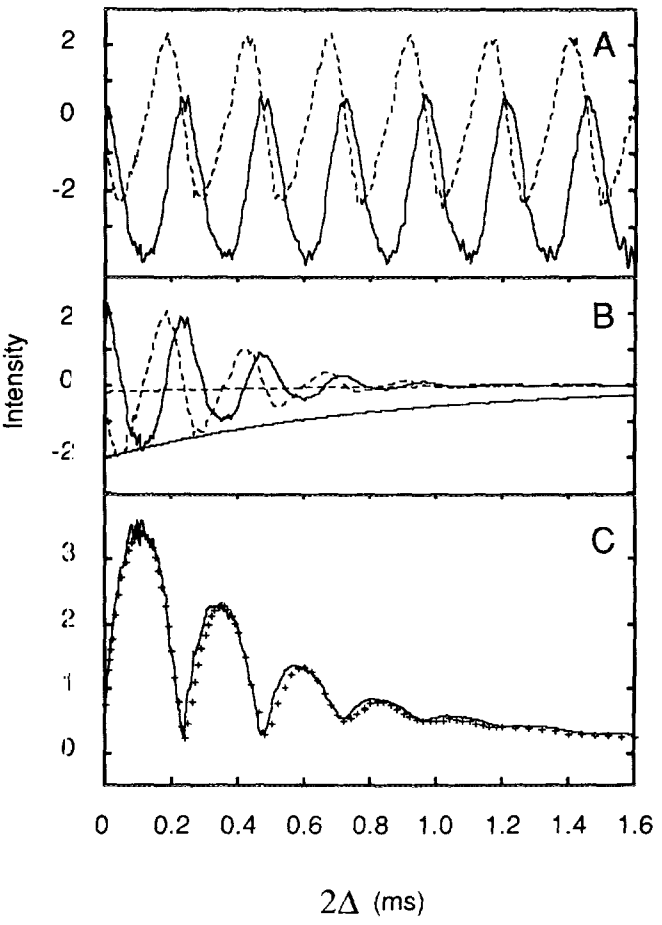

FIG. 6. Spin-echo NMR intensity results for hydrated Linde Y, at 23°C. (A) Real and imaginary part of the spin-echo amplitude, $E_{-1/2,1/2}(2\Delta) \times 35$, as a function of the pulse separation, Δ. The in-phase pulse sequence used had $\omega_{RF}\tau_1 = \pi/6$, $\omega_{RF}\tau_2 = \pi/3$, with $\omega_{RF} = (2\pi)27.8$ kHz; $\nu_Q = 270$ kHz, $\eta = 0.5$; resonance offset, $\delta\omega = (2\pi)8.2$ kHz. (B) $E_{-1/2,1/2}(2\Delta)$ is separated into two components: the oscillations, $E_0 = E_{-1/2,1/2}(2\Delta) - \bar{E}_{-1/2,1/2}(2\Delta)$, and the time average, $E_c = \bar{E}_{-1/2,1/2}(2\Delta)$. E_0 is assumed to decay with $T_2 \approx 240$ μs (20% Lorentzian, 80% Gaussian); E_c is assumed to decay with $T_{2E} = 800$ μs (100% Lorentzian). (C) +, experimental ^{27}Al NMR spin-echo decay of hydrated NaY [cf. Fig. 4 (●)]. The solid line is the numerical fit, $|E_0 + E_c|$, from B.

phase-corrected Fourier-transformed spectra of the spin echoes, with $t \geqslant 2\Delta$. As can be seen from Fig. 6C, this approach fits the experimental spin-echo decay very well. In addition, since the oscillations are a measure of the quadrupole interaction at a given RF field, the quadrupole interaction itself can be estimated. In the zeolite NaY example shown, we find $\nu_Q = 270 \pm 30$ kHz, in good accord with the results of others (*20*).

If, for $\Delta \gg T_2$, a spin echo can still be observed ($T_{2E} \gg T_2$), it follows from the explanation above that the influence of the second free induction decay vanishes and only the refocused component (spin echo) is observed, but with a smaller amplitude.

For a 90°-phase-shifted pulse sequence, with partially selective pulses according to Eq. [35], the experimentally observed spin-echo decay is now the superposition of a spin-echo decay and a 90°-phase-shifted free induction decay. In an on-resonance experiment, the signal at $t = 2\Delta$ is typically larger than that seen with an in-phase echo sequence, since for an in-phase sequence and weak excitation of the satellite transitions, the second free induction decay and the spin echo are phase shifted by 180°. In an off-resonance experiment, essentially the same oscillatory behavior as that with the in-phase sequence is observed; however, the phase of the oscillations is now shifted by 90° compared to the results shown in Fig. 6.

In conclusion, our results indicate that considerable care needs to be taken in order to obtain accurate spin-echo NMR quantitation of non-integral-spin quadrupolar nuclei in solids. While nonselective excitation has none of the problems associated with partially selective excitation, it is rarely achievable in real systems. Thus, selective excitation is generally essential for reliable quantitative work, and low power levels are required—in the results described above, typical "solid" 90° pulse widths were in the range 40–70 μs, although somewhat higher power levels may be acceptable in some cases. For much higher power levels, satellite-transition excitation complicates data analysis, but if ν_Q is known, it can be accounted for. In addition, off-resonance excitation causes complex oscillatory echo decays; however, ν_Q can be estimated from such data, by using numerical methods.

The ability to remove rapidly decaying signals using weak spin-echo excitation while maintaining the ability to determine quantitatively framework zeolite levels in real-world catalysts is an obvious, but nonetheless useful, application of the methods outlined above (*21*).

ACKNOWLEDGMENT

We thank Dr. K. D. Schmitt for informing us of the results of his resonance-offset experiments.

REFERENCES

1. E. Oldfield and R. J. Kirkpatrick, *Science* **227,** 1537 (1985).
2. J. Haase and E. Oldfield, *J. Magn. Reson. Ser. A* **101,** 30 (1993).
3. J. Haase, K. D. Park, K. Guo, H. K. C. Timken, and E. Oldfield, *J. Phys. Chem.* **95,** 6996 (1991).
4. D. Fenzke, D. Freude, T. Fröhlich, and J. Haase, *Chem. Phys. Lett.* **111,** 171 (1984).
5. D. Massiot, C. Bessada, J. P. Coutures, and F. J. Taulelle, *J. Magn. Reson.* **90,** 231 (1990).
6. V. H. Schmidt, *in* "Pulsed Magnetic and Optical Resonance" (R. Blinc, Ed.), Proceedings of the Ampere International Summer School II, Basko polje, 2–13 September 1971, pp. 75–83, University of Ljubljana, Ljubljana, Yugoslavia, 1972.
7. P. P. Man, J. Klinowski, A. Trokiner, H. Zanni, and P. Papon, *Chem. Phys. Lett.* **151,** 143 (1988).
8. N. C. Nielsen, H. Bildsøe and H. J. Jakobsen, *Chem. Phys. Lett.* **191,** 205 (1992).
9. U. Haeberlen, "High Resolution NMR in Solids, Selective Averaging," Academic Press, New York, 1976.
10. M. E. Rose, "Elementary Theory of Angular Momentum," Wiley, New York, 1967.
11. A. Abragam, "Principles of Nuclear Magnetism," Oxford Univ. Press, Oxford, 1961.
12. A. Samoson and E. Lippmaa, *Phys. Rev. B* **28,** 6567 (1983).
13. R. P. Feynman, *Phys. Rev.* **84,** 108 (1951).
14. K. Kambe and J. F. Ollom, *J. Phys. Soc. Jpn.* **11,** 50 (1956).
15. P. Mansfield, *Phys. Rev. A* **137,** 961 (1965).
16. J. Haase, D. Freude, H. Pfeifer, E. Lippmaa, and P. Sarv, *Chem. Phys. Lett.* **152,** 254 (1988).
17. R. V. Pound, *Phys. Rev.* **79,** 685 (1950).
18. J. Haase, E. Oldfield, and K. Schmitt, *Chem. Phys. Lett.* **193,** 274 (1992).
19. J. Haase and H. Pfeifer, *J. Magn. Reson.* **86,** 217 (1990).
20. E. Lippmaa, A. Samoson, and M. Mägi, *J. Am. Chem. Soc.* **108,** 1730 (1986).
21. K. D. Schmitt, J. Haase, and E. Oldfield, unpublished results.